Volume 70 • Issue 2 • June 2015

Journal of Achievements in Materials and Manufacturing Engineering

International Scientific Journal published monthly by the World Academy of Materials and Manufacturing Engineering

Corrosion testing of nickel alloy for molten salt reactors

P. Slama [a,*], M. Marecek [b]

[a] COMTES FHT a.s., Prumyslová 995, 334 41 Dobrany, Czech Republic

[b] Research Centre Rez, Hlavni 130, Rez, 250 68 Husinec, Czech Republic

* Corresponding e-mail address: peter.slama@comtesfht.czl

ABSTRACT

Purpose: The article deals with corrosion test conducted in LiF – BeF_2 molten salt at 700°C using nitrogen as the inert atmosphere with the test durations of 1 and 3 months.

Design/methodology/approach: The experiment was carried on nickel superalloy MoNiCr which was developed by COMTES FHT Inc. for application in molten salt reactors circuits. Corrosion testing was conducted in collaboration with Nuclear Research Institute Rez.

Findings: The results show that chromium and molybdenum are preferentially released into the melt and the surface and grain boundaries become depleted of chromium.

Rerearch implications: The assessment of corrosion damage suggests that in the LiF-BeF_2 melt at 700°C, chromium and molybdenum are preferentially released into the melt and the surface and grain boundaries become depleted of chromium.

Originality/value: The nickel alloys are determined for modern conceptions of nuclear reactors in which molten fluoride salts are used in the primary and/or secondary circuit as coolants. Particularly MONICR alloy represents a material alternative with high corrosion resistance in the area of fluoride salts and it has very good creep properties in the temperature range of 650-750°C as well.

Keywords: Nickel alloys; Salt reactors; Fluorite salts; Corrosion

Reference to this paper should be given in the following way:

P. Slama, M. Marecek, Corrosion testing of nickel alloy for molten salt reactors, Journal of Achievements in Materials and Manufacturing Engineering 70/2 (2015) 78-85.

PROPERTIES

1. Introduction

The superalloys are nickel-, iron-nickel-, and cobalt-base alloys generally used at temperatures above about 540°C. The iron-nickel-base superalloys are an extension of stainless steel technology and generally are wrought. A large number of alloys have been invented and studied; many have been patented. However, the many alloys have been winnowed down over the years; only a few are extensively used [1]. Due to their excellent creep resistance nickel based superalloys are predestined for the power industry, especially for power engineering. [1]

Current nuclear power engineering is mostly represented by light-water nuclear reactor which uses low-enriched uranium in the form of uranium dioxide as their fuel. However the current use of a uranium raw material is low, in most cases it ranges between 3 and 5%. The limited number of reactors uses mixed uranium-plutonium fuel which increases the primary use of the uranium raw

material. The research of fourth type reactors system deals with the way how to prevent from non-economical uranium exhaustion [2]. The fourth generation of reactors is generally divided into two types: thermal and fast reactors. Thermal reactors use the moderator to slow the neutrons emitted by fission to make them more likely to be captured by the fuel. A fast reactor directly uses the fast neutrons emitted by fission, without moderation. These new reactors are designed with the following objectives in mind [2 - 4]:

- Enhanced nuclear reactors safety
- Increase in nuclear reactors energy efficiency
- Closure of nuclear reactors fuel cycle
- Reducing spent fuel radioactivity level
- Disposal with spent fuel

It appears that waste management is a major concern with the existing once-through cycle because of the limited availability of repository space worldwide. Closed fuel cycles of recycling reactors allow some of the fuel to be reused. Improvement in reactor performance can be achieved if thermal and fast reactors are operated in a coupled mode. An increase in the fuel burnup of thermal reactors can improve the management of the produces actinides by burning them in situ. With transmutation, the relative toxicity of radioactive waste considerably decreases [4]. Increase in nuclear power plants energy efficiency is possible by increasing the output coolant temperature in the reactor. It can be reached if a different coolant from water is used. Sodium, lead, gases, supercritical water and other media are under consideration. One of the conceptions for the fourth generation reactors is a molten salt reactor where molten fluoride salts medium is considered in the primary and also in the secondary circuit. Main advantage of this reactor type is high efficiency (high level of nuclear fuel use), but the main disadvantage is the environment of molten fluoride salts with temperature 700 – 800°C. A suitable material for fittings and vessels must bring extreme corrosive and creep resistance in this environment. [5]

The main microstructure parameter which affects the mechanical properties and also creep resistance is the grain size. Grain size greatly influences strength, creep, fatigue crack initiation and growth rate. The uniform coarse grain size increases creep strength, crack growth resistance and ductility. Contrary, the uniform fine grain size provides a high-low cycle fatigue life and high tensile and yield strength [6]. Numerous previous studies were focused on reaching of microstructure with uniform grain by means of thermomechanical processing [2,3].

Many studies stated that nickel based superalloys materials with high Mo and low Cr contents are generally superior in high temperature corrosion resistance in fluorine environments [5]. The effort to find the ideal chemical composition is spent from the 1950s, when extensive testing began in the USA in Oak Ridge National Laboratory (ORNL). First studies showed, that Ni based alloys exhibit the best corrosion resistance in molten fluorides. Actually, pure nickel is the best material in this point of view, but cannot be used alone. Nickel itself is too soft at the working temperature of the reactor and its creep resistance is negligible.

Conventional Ni-based superalloys are meant to be used at high temperatures, under stress and in the corrosive environment (especially oxidating). The creep resistance of these commonly used superalloys comes either from intermetallic phase precipitation (γ' phase Ni3(Al,Ti)) or from solid solution strengthening. Intermetallic phases are severely attacked by fluoride salts. Hence, only solid solution strengthening is applicable for this environment. It is achieved (in common oxidation resistance) is usually achieved by high chromium (from 15 to 30 wt.%) and iron content. Both of these elements are depleted from the alloy during fluoride salt exposition so that the chromium content has to be lowered to the minimum acceptable level for the alloy passivation at the high temperature in air and iron should be excluded at all.

The corrosion tests are usually conducted in sealed graphite or alumina capsules, placed for desired period of time in the furnace. Capsules are filled with fluoride salt mixture (most promising are compositions LiF-BeF or LiF-NaF-KF) and the sample is placed in. Salt purity is crucial for the corrosion rate. The salts are specially treated to remove any impurities, especially water and distributed in sealed containers. The Capsules filling is conducted above the melting point of the salt under inert atmosphere [6].

More advanced corrosion tests simulate the reactor cooling circuit by thermal convection loop. Tested material is shaped into tubing and joined to form a loop with one vertical leg heated and the second vertical leg cooled. Natural convection then ensures molten salt circulation in the loop, so that the motion of the corrosive medium and temperature gradients are included in test layout [7, 8].

Table 1.
Chemical composition of experimental alloy

Element	Mo	Cr	Ti	Fe	Mn	Nb	Al	W	Ni
Wt. %	15.81	6.82	0.03	2.32	0.04	0.01	0.26	0.06	base

2. Corosion testing

The experiment was carried on nickel superalloy MoNiCr which was developed by COMTES FHT Inc. for application in molten salt reactors circuits. The chemical composition of this alloy is shown in Table 1.

Corrosion testing was conducted in collaboration with Nuclear Research Institute Rez. The specimens were metal sheets with the size of 18x40 mm and approx. 1.2 mm thickness. Prior to testing, the specimens were placed in closable graphite containers (in order to prevent the molten mass from reacting with the material of the vessel). A total of three corrosion tests (specimens no. 6, 7 and 8) were conducted in LiF - BeF_2 molten salt at 700°C using nitrogen as the inert atmosphere with the test durations of 1 and 3 months.

Corrosion Test of Specimen No. 6: Test Period of 1 Month

The specimen no. 6 was placed in a closable threaded-lid graphite container with molten LiF-BeF_2 (the charge: 11.47 g BeF_2 and 12.31 g LiF). The one-month test took place at 700 °C in an inert atmosphere consisting of nitrogen. The weight of the specimen after removal from the container and after cleaning was 6.3628 g (the weight loss was 0.6356%) (note: the weight loss in specimen no. 5 (three-month test) was 5.6%).

Corrosion Test of Specimen No. 7: Test Period of 3 Months

The specimen no. 7 was placed in a closable threaded-lid graphite container with molten LiF-BeF_2 (the charge: 8.5 g BeF_2 and 9.13 g LiF). The long-term test took place at 700 °C in an inert atmosphere consisting of nitrogen. The weight of the specimen after removal and cleaning was 7.7878 g (the weight loss was 1.9391%).

Corrosion Test of Specimen No. 8: Test Period of 1 Month

Sspecimen no. 8 was cut to the required size (thickness: 1.14-1.19 mm, width: 18.07-18.11 mm, length: 24.89-24.91 mm) and then it was placed in a closable threaded-lid graphite container (1) containing molten LiF-BeF_2 (the charge: 10.42 g BeF_2, 11.65 g LiF). The one-month test took place at 700 °C in an inert atmosphere consisting of nitrogen. Throughout the corrosion test, the entire specimen was submerged in the melt.

The weight of the specimen after removal and cleaning was 4.5295 g (representing the weight loss of 2.4277 %). Specimen dimensions after the experiment: thickness: 1.11-1.19 mm, width: 18.04-18.08 mm, length: 24.90-24.91 mm.

a) Graphite containers

b) Graphite containers in dry box

c) MoNiCr specimen no. 6 in solidified salt after the experiment<0}

Fig. 1. Specimen arrangement and specimen no. 6 after testing

The only variation in the corrosion test conditions was the duration of the exposure of the nickel alloy to the LiF-BeF_2 molten salt. In addition, the size of the specimen no. 8 was altered to allow the specimen to be fully submerged in the molten salt during the experiment. All tests were conducted at 700°C in an inert atmosphere of nitrogen (Table 2).

Table 2.
Overview of corrosion tests

MoNiCr specimen number	Specimen no. 6	Specimen no. 7	Specimen no. 8
Temperature [°C]	700	700	700
Corrosion test duration	1 month	3 months	1 month
Atmosphere:	N_2	N_2	N_2
Specimen submerged	Partially	Partially	Fully
Corrosion loss [%]	0.64	1.94	2.43

In order to obtain more accurate evaluation of corrosion tests, it is advisable to conduct experiments in which the specimens are fully submerged in the molten salt. With specimens only partially submerged in the melt, the area attacked by the molten salt (LiF-BeF_2) is impossible to determine accurately, preventing a clear evaluation of the corrosion loss. Nevertheless, the corrosion losses in specimen nos. 6 and 7 allow some comparison, since graphite containers of identical sizes, specimens of identical dimensions and similar amounts of molten salt were used in the tests.

3. Analysis of LiF-BeF_2 melt by means of ICP-MS

After the exposure, specimens of solidified salt were supplied to Central Analytic Laboratory of ÚJV Řež a.s., where they were dissolved and the solutions measured using the ICP-MS method. The analysis focused on levels of metals (nickel, chromium, molybdenum and iron) in the melt. Results of the analysis conducted by the Central Analytic Laboratory are given in the following table 3.

The results suggest that the metals which were rapidly released from MoNiCr alloy into the melt were chromium and molybdenum. The results showed that the melt in the corrosion test of the specimen no. 6 was contaminated with iron and, possibly, a small amount of chromium, which is why the percent levels of the other metals are lower. The results of melt analysis and the corrosion loss data were used for calculating the complete mass balance of the elements of interest, but its results were ambiguous. It might be attributed to the distribution of the analysed metals in the melt which was not quite uniform.

Table 3.
Results of analysis of water solutions obtained by leaching the cleaned specimens

MoNiCr specimen number	Element	Element content µg/g specimen	Expanded standard uncertainty µg/g specimen
6	Cr	141.560	7.078
	Fe	48.299	2.415
	Mo	112.016	5.601
	Ni	123.587	6.179
7	Cr	59.212	2.961
	Fe	<0.050	0.003
	Mo	93.220	4.661
	Ni	79.774	3.989
8	Cr	32.645	1.632
	Fe	<0.050	0.003
	Mo	103.487	5.174
	Ni	61.502	3.075

4. Observation of specimens after corrosion testing

After removing the corrosion products, the surface of the specimens was documented, including scanning electron micrographs. Transverse metallographic sections were prepared for examining the attacked surface using optical and scanning electron microscopy and EDS analysis. The surfaces of specimens after corrosion testing and after removal of corrosion products are shown in Fig. 2.

The parts of specimens 6 and 7 with the hole were not submerged in the melt during testing. It can be seen that the chosen method of removing corrosion products is very effective in cleaning the surface. The surfaces of specimens were also photographed using SEM. The micrographs are shown in Fig. 3.

a) Specimen 6

b) Specimen 7

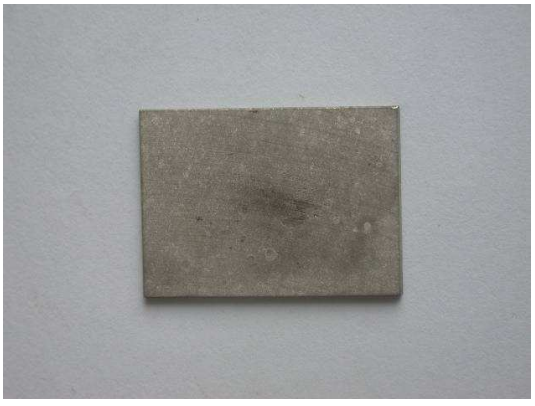

c) Specimen 8

Fig. 2. Surface of specimens after removal of corrosion products

At some locations on the specimens, notable attack on grain boundaries (intergranular corrosion) can be observed.

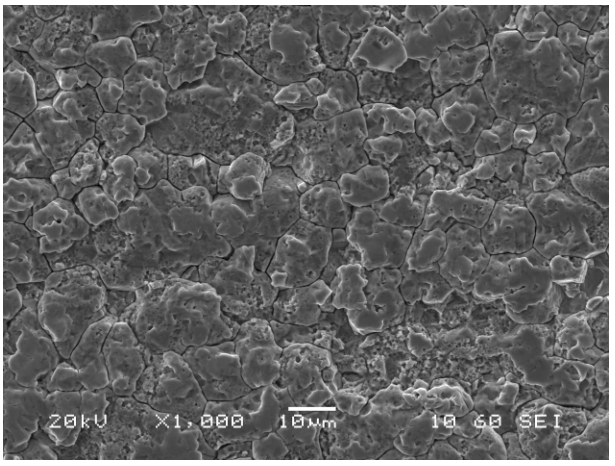

a) Specimen 6

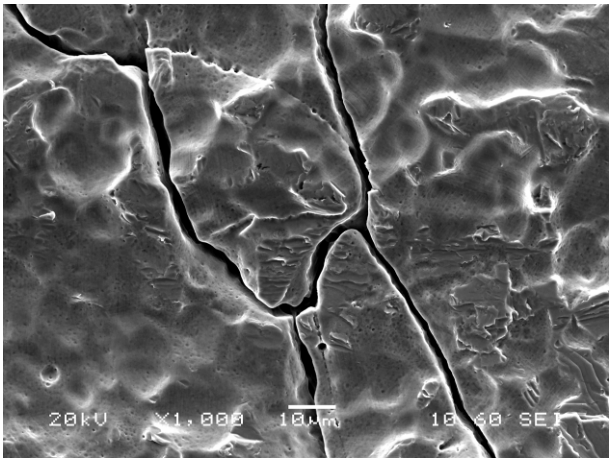

b) Specimen 7

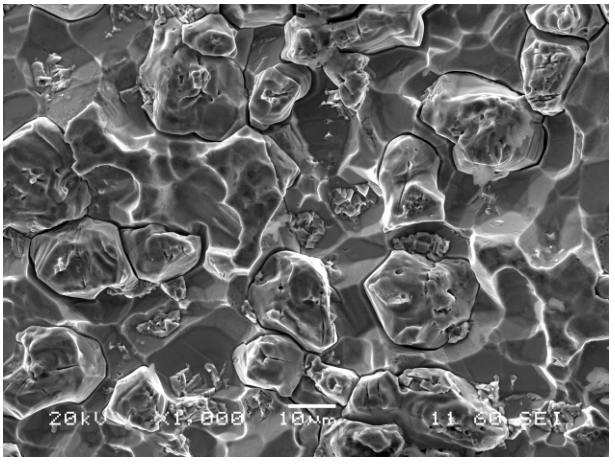

c) Specimen 8

Fig. 3. Scanning electron micrographs of specimen surfaces after corrosion testing

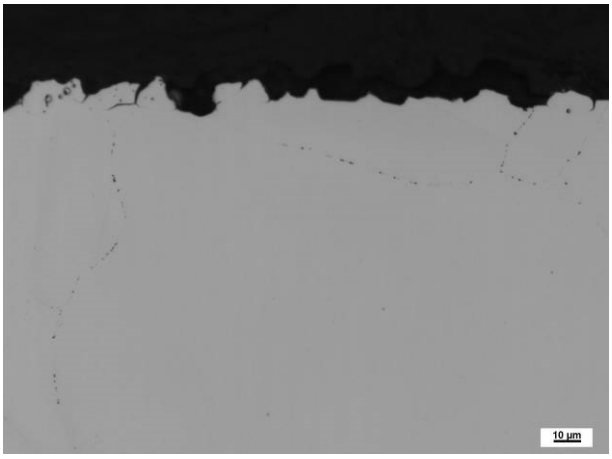

a) Specimen 6, magnification 500x

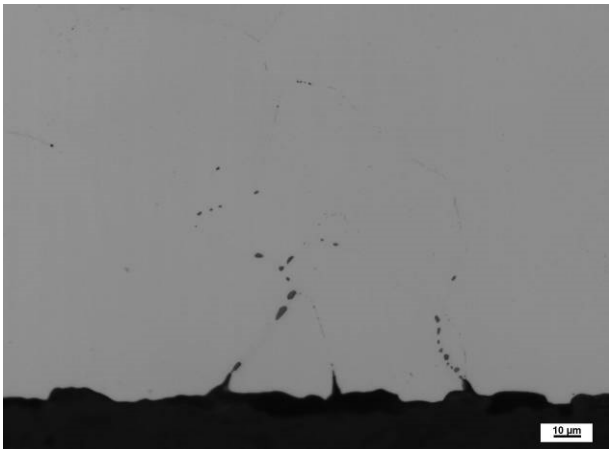

b) Specimen 7, magnification 500x

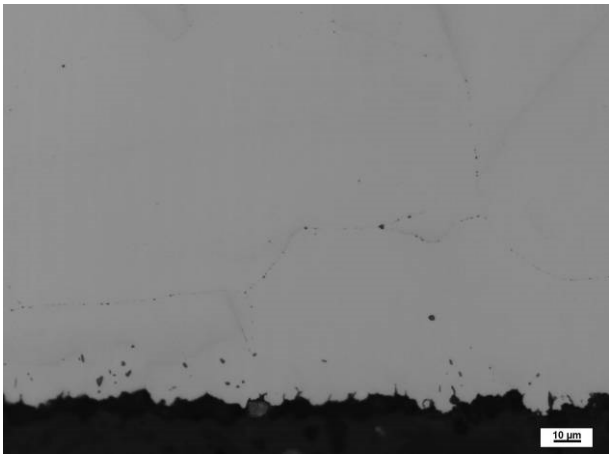

c) Specimen 8, magnification 500x

Fig. 4. Microstructures of specimens near the surface. Unetched condition

The microstructures of specimens after corrosion testing observed on their transverse cross-sections.

In no. 6, the specimen thickness was measured in the submerged part (end of the specimen) and in a location near the hole which was not submerged in the melt. The readings were used for calculating the thickness loss after the corrosion test. The measured values and the calculated thickness loss are shown in Table 3.

Table 3.
Thickness and thickness loss in specimen no. 6 [µm]

Location	End	Hole	Loss in µm	Loss in %
Part A	973.1	986.95	13.85	1.40
Part B	971.85	981.92	10.07	1.03

This value is slightly higher than the weight loss which was 0.64 %. However, the weight loss measurement did not account for the fact that only part of the specimen was submerged in the melt. Following figures show the corrosion attack of the specimen surface.

The micrographs mostly show uniform corrosion. Grain boundaries were attacked in some locations. In those, precipitates can be found along grain boundaries.

EDS analysis of specimens after corrosion testing

EDS analysis of locations near the specimen surface was performed using scanning electron microscope JEOL 6380 with EDS detector INCA x-sight. Results of the EDS analysis of particles near the surface of specimen no. 7 are shown in Fig. 5.

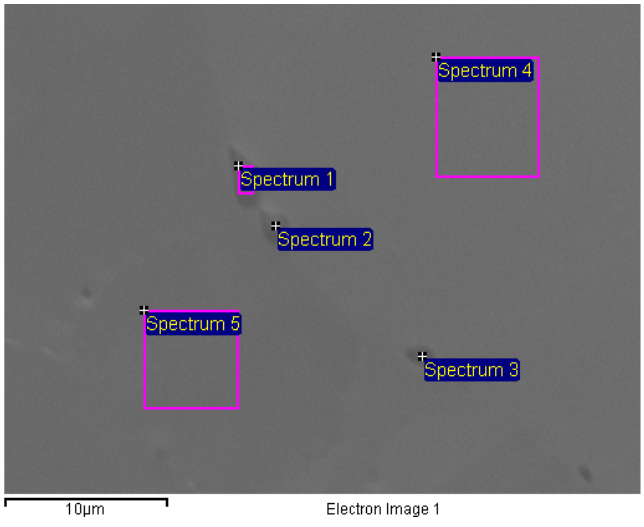

Fig. 5. EDS analysis of specimen no. 7

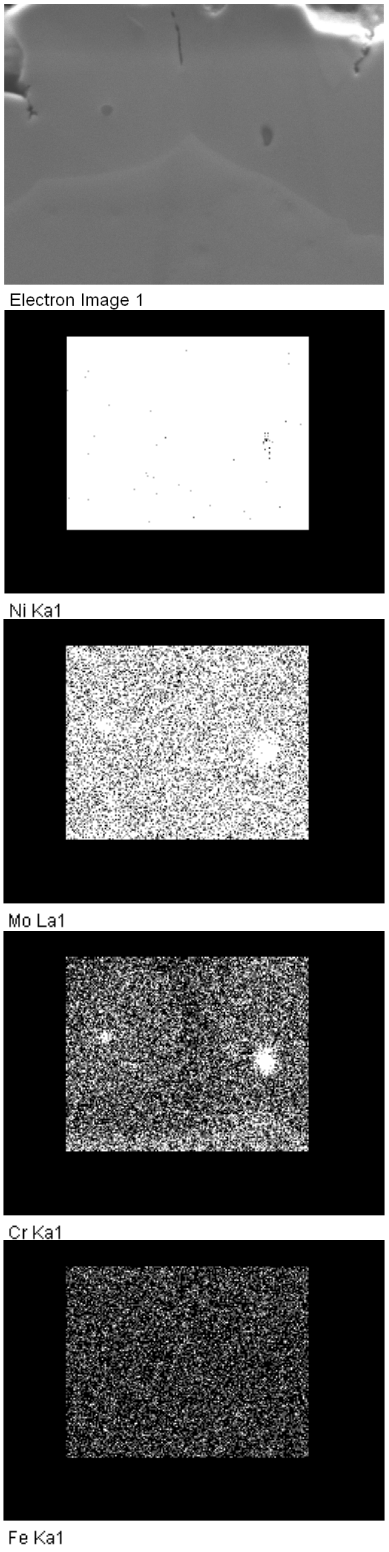

Fig. 6. X-ray maps for elements near the surface of specimen no. 6

Table 4.
EDS analysis [wt.%]

Spectrum	Cr	Fe	Ni	Mo
Spectrum 1	35.39	0.33	12.06	52.22
Spectrum 2	29.39	0.59	23.31	46.71
Spectrum 4	5.98	1.41	77.03	15.58
Spectrum 5	6.11	1.37	76.70	15.82

The EDS analysis showed that the particles near the attacked surface (1 and 2) have considerably higher Mo and Cr content than the base material. According to the Cr-Mo phase diagram, the system contains no intermetallics. Both metals are completely soluble. It is more likely to be a ternary phase formed due to long annealing at the corrosion test temperature of 700 °C.

Also the element map (see fig. 5) shows particle with higher molybdenum and chromium levels and suggests that the grain boundaries are depleted of chromium. Similar chromium depletion was detected in specimen 7. According to the image, grain boundaries are depleted of chromium and the particles have higher levels of molybdenum and chromium.

5. Conclusion

Corrosion tests on three specimens of MoNiCr-type nickel alloy were conducted. The only variation in the corrosion test conditions was the duration of the exposure of the nickel alloy to the LiF-BeF_2 molten salt. In addition, the size of the specimen no. 8 was altered to allow the specimen to be fully submerged in the molten salt during the experiment. All tests were conducted at 700°C in an inert atmosphere of nitrogen. The assessment of corrosion damage suggests that in the LiF-BeF_2 melt at 700°C, chromium and molybdenum are preferentially released into the melt and the surface and grain boundaries become depleted of chromium. Particles with elevated levels of molybdenum and chromium were found on grain boundaries.

Acknowledgements

These results were created under the project entitled Development of West-Bohemian Centre of Materials and Metallurgy No.: LO1412, financed by the Ministry of Education, Youth and Sports of the Czech Republic.

This work has been supported by the SUSEN Project CZ.1.05/2.1.00/03.0108 realised in the framework of the European Regional Development Fund (ERDF).

References

[1] M.J. Donachie, S.J. Donachie, A. Superalloys, Technical Guide, The Materials Information Society, Materials Park, OH 44073-0002, 2002, ISBN 0-87170-749-7.

[2] Z. Novy, J. Dzugan, P. Motycka, P. Podany, J. Dlouhy, On Formability of MoNiCr Alloy, Advanced Materials Research 295-297 (2011) 1731-1737. www.scientific.net/AMR.295-297.1731

[3] Z. Novy, J. Dzugan, P. Wangyao, L. Kraus, Development of Forming Processes for MoNiCr Alloy, Key Engineering Materials 658 (2015) 3-7.

[4] 2014 GIF Annual report. Available at: http://tinyurl.com/GIF2014-annual-report

[5] P. Wang Yao, et al., Microstructure Development by Hot and Cold Working Processes in Nickel Based Alloy, Journal of Metals, Materials and Minerals 13/2 (2000) 333-43.

[6] Zheng Guiqiu, Corrosion Behavior of Alloys in Molten Fluoride Salts, dissertation thesis, 2015, University of Wisconsin-Madison.

[7] N. Iwamoto, Y. Makino, K. Furukawa, Y. Katoh, H. Katsuta, Corrosion of the Hastelloy-N in Molten Flinak Loop, Transactions of JWRI 9/2 (1980) 259-261.

[8] J.W Koger, Corrosion Product Deposition in Molten Fluoride Salt Systems, Oak Ridge National Laboratory, Oak Ridge, Tenessee, 1973.